

Application of radio tomographic imaging to HF oblique incidence ray tracing

N. C. Rogers,¹ C. N. Mitchell,^{2,3} J. A. T. Heaton,¹ P. S. Cannon,¹
and L. Kersley²

Abstract. Radio tomography is a technique for generating images of the spatial structure of ionospheric electron density over a wide area. This paper assesses the potential use of radio tomography in HF oblique propagation and ray tracing applications. Synthetic ionograms produced by ray tracing through tomographic images and ionospheric models have been compared with experimental oblique ionograms from six paths lying close to the image plane in the United Kingdom. In particular, study has been made of the effects of various types of input information used to constrain the vertical electron density structure in the tomographic reconstructions. It was found that use of a fine height resolution (5 km) and incorporation of information from one vertical ionosonde in the reconstruction process makes significant improvements to the overall reliability of the tomographic image. As expected, *E* layer propagation is better defined using a climatological model than by tomography. However, in comparison with three ionospheric models, use of tomographic images can significantly reduce the RMS error in the determination of the F_2 layer maximum usable frequency.

1. Introduction

Wide area imaging of ionospheric electron density is important for both geophysics research and radio system operation. There are a number of complementary techniques, which can be used to achieve this. While scans by incoherent scatter radars can provide images of the ionosphere, widespread use of the technique is limited by cost. Networks of ionosondes can also be used to generate information about the ionosphere over wide areas, and they are relatively inexpensive. However, ionosondes are unable to image above the height of peak electron density and are often subject to *D* region absorption, blanketing sporadic *E* layers, and scattering of the returned signals. Interpolation between the discrete measurements is also subject to considerable error. Radio tomography is an approach that provides high-resolution images of ionospheric electron concentration, both above and below the *F* region peak over an

extended spatial region. Using passive reception of transmissions from satellites in low Earth orbit, the technique is relatively inexpensive, and interpolation within or close to the orbital plane is not a problem.

Tomographic images are produced by determining the total electron content (TEC) (integrated electron density) along satellite-ground paths by measuring the phase difference between two phase-locked radio transmissions from a satellite in polar orbit. A chain of tomography receivers situated approximately along the meridional orbital plane is used to measure the TEC on a large number of intersecting paths from which a two-dimensional image of electron density may be reconstructed. Reference to recent work on radio tomographic imaging is given by *Kersley et al.* [1997] and *Pryse et al.* [1998], and a wider review is given by *Leitinger* [1999].

Ionospheric tomography is a “limited angle” technique since few rays cross the ionosphere at shallow angles of incidence. In consequence, certain a priori conditions must be used to constrain the vertical profile in the reconstruction process. Furthermore, use of additional input information from ionosondes has been shown to aid the imaging procedures.

For radio systems applications it is important that the accuracy of the ionospheric ray tracing be well matched to the electron density specification. For high-accuracy numerical and analytic ray tracing, ionospheric tomography may provide that high-accu-

¹ Defence Evaluation and Research Agency, Malvern, Worcestershire, England, United Kingdom.

² Department of Physics, University of Wales, Aberystwyth, Wales, United Kingdom.

³ Now at the Department of Electronic and Electrical Engineering, University of Bath, Bath, England, United Kingdom.

racy electron density specification. In this paper, the accuracy of the tomographic image reconstruction for various a priori preconditions is assessed. The experimental study involved comparison of oblique incidence (OI) ionograms recorded on paths lying close to the plane of the tomographic receiver chain with synthetic OI ionograms produced by ray tracing through the tomographic images. In addition, ray tracing was performed through model ionospheres, and the results were compared to experimental OI ionograms.

Until recently, accurate ray tracing through a potentially complex ionosphere represented by the tomographic image would have been achieved using relatively slow numerical programs. However, *Norman and Cannon* [1997, 1999] have developed a fast, analytical technique to trace through horizontally structured ionospheres. The method offers a tenfold to one hundredfold speed improvement over the numerical methods with only a slight loss of accuracy (typically less than 4% ground range error) (Rogers et al., unpublished technical report, 1998). The method is based on dividing the ionosphere vertically into multiple quasi-parabolic segments, for which analytical solutions are available [*Dyson and Bennett*, 1988], and horizontally into sectors using the segmented method for analytical ray tracing (SMART). The technique has recently been enhanced to facilitate ray tracing through tomographic images.

2. Experimental Arrangement

A chain of five TEC automated receiving stations in the United Kingdom was operated by the University of Wales, Aberystwyth, between October 1997 and October 1999. The chain extended over 10° of latitude from Dartmouth (50.3°N) to Saxa Vord (60.8°N) (Figure 1). Signals were recorded on a routine basis from the Naval Ionospheric Monitoring System (NIMS) satellites, which orbit at approximately 1100 km altitude.

Ionosondes at Chilton (51.5°N , 1.3°W) and Lerwick (60.2°N , 1.2°W) (Figure 2) recorded vertical incidence (VI) ionograms at 30 min intervals. These ionograms were used to infer the electron density profile above each station (up to the peak of the *F* region ionosphere) using the polynomial analysis (POLAN) inversion procedure [*Titheridge*, 1979, 1985]. Ionograms recorded within 15 min of a satellite pass were inverted and used as a priori information to guide the tomographic reconstruction.

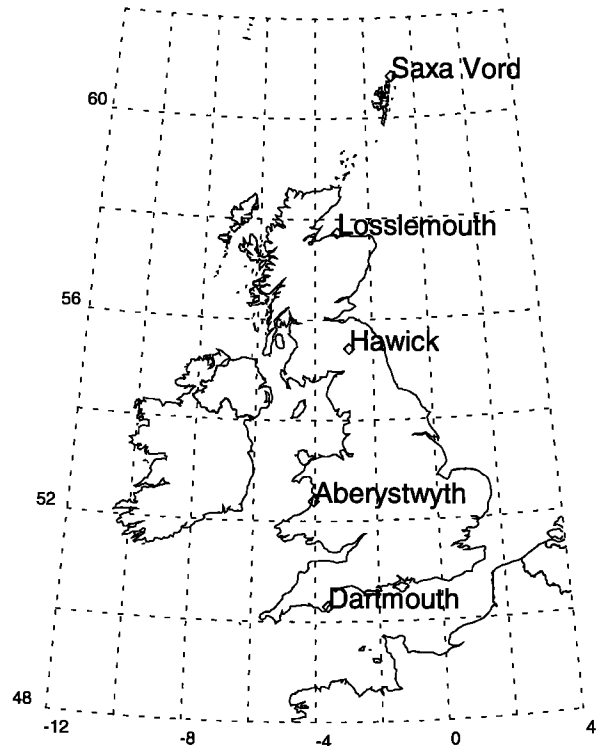


Figure 1. Map showing the locations of the tomography receivers at Saxa Vord (60.8°N), Lossiemouth (57.7°N), Hawick (55.4°N), Aberystwyth (52.5°N), and Dartmouth (50.3°N).

OI ionograms were recorded over six United Kingdom paths using the “Improved Radio Ionospheric Sounder” (IRIS) system [*Arthur et al.*, 1997] (Figure 2). The IRIS sounder incorporates GPS satellite timing synchronization to permit the measurement of absolute rather than relative group path delays.

3. Tomographic Reconstructions

For the tomographic reconstructions, absolute TEC was estimated using a multistation development of the least squares calibration method described by *Leitinger et al.* [1975]. Compensation for the longitude difference between the satellite and the receiver was made using a cosine correction at the zenith angle of the ray path at 350 km altitude during nighttime and 280 km during the day. The tomographic images have been reconstructed using a derivative of the discrete inverse theory (DIT) method described by *Fremouw et al.* [1992], with an orthogonal basis set of functions formed from a range of Chapman profiles created to

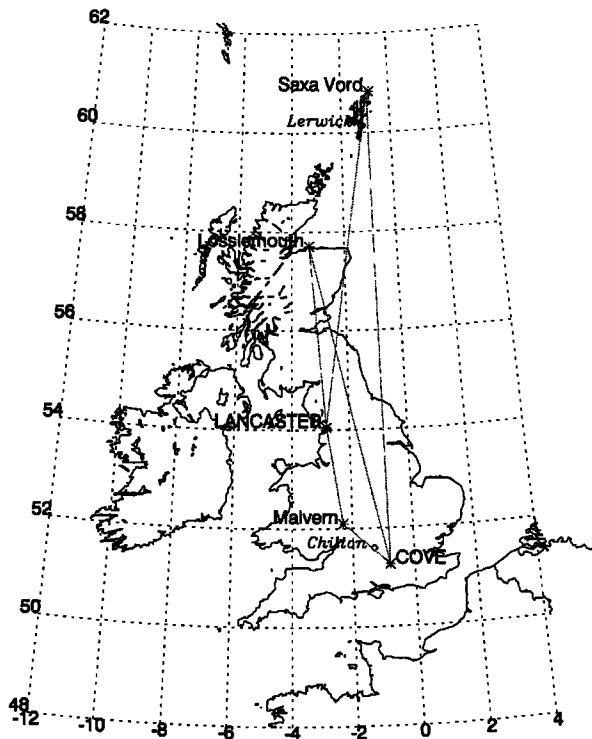


Figure 2. Map of transmitters (uppercase), receivers (lowercase), and great circle propagation paths of the IRIS oblique sounder network. Locations of VI ionosondes at Chilton and Lerwick are also indicated in small italics.

cover appropriate peak and scale heights. The DIT procedure reconstructs the large-scale features in the ionosphere while subsequent processing by the algebraic reconstruction technique (ART) is used to form the smaller-scale density structures, to 0.25° latitudinal resolution.

4. Ray Tracing Through Tomographic Images and Model Ionospheres

A homing procedure, described by *Rogers et al.* [1999], was incorporated into the SMART ray tracing algorithms such that synthetic oblique ionograms could be produced through various tomographic and model specifications of the ionosphere. Five variants of the DIT-ART tomographic reconstruction procedure were examined. These methods are labeled A to E and summarized diagrammatically in Table 1. In method A the grid of electron densities was created at 15 km height intervals and the algorithm incorporated electron density profiles derived from VI ionograms recorded at Chilton. Method B used a finer height resolution of 5 km while still incorporating Chilton data. In method C, electron density profiles derived from both Chilton and Lerwick ionograms were incorporated while still retaining the fine height resolution. Both methods D and E reconstructed the tomographic image at 5 km height intervals, but neither made use of ionosonde measurements. Methods A to D included Chapman functions representing both the *E* and *F* regions in the set of orthonormal functions used in the tomographic reconstruction algorithm, but method E was unique in that the Chapman functions used represented only the *F* region profile. In general, the electron density was extrapolated to a zero base at a height of 80 km.

Times were identified when experimental OI ionograms were available within 10 min of satellite passes for which the maximum elevation of the ray path was greater than 80° . This condition was imposed to ensure that the tomographic images were representative of the ionosphere over the U.K. IRIS paths

Table 1. Summary Description of the Variants Used in the Tomographic Reconstructions

Tomographic Reconstruction Method	Height Interval, km	A priori Electron Density Profile	Chapman Function Representation
A	15	POLAN inversion of Chilton ionogram	both <i>E</i> and <i>F</i> regions of the ionosphere
B	5	POLAN inversion of Chilton ionogram	both <i>E</i> and <i>F</i> regions of the ionosphere
C	5	POLAN inversion of both Chilton and Lerwick ionograms	both the <i>E</i> and <i>F</i> regions of the ionosphere
D	5	no sounder information	both <i>E</i> and <i>F</i> regions of the ionosphere
E	5	no sounder information	only the <i>F</i> region; no representation of the <i>E</i> region

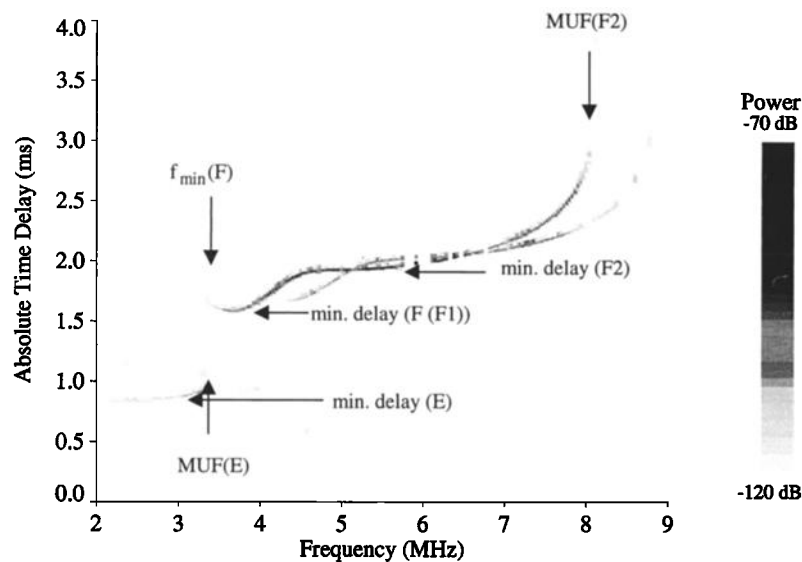


Figure 3. IRIS oblique ionogram for the Cove-Malvern path on April 2, 1998, at 1516 UT. The six scaled parameters ($f_{\min}(F)$, $MUF(E)$, $MUF(F_2)$, $m'd(E)$, $m'd(F_1)$, and $m'd(F_2)$) are indicated.

(rather than to the east or west). Each tomographic image was then extended uniformly in longitude to produce a three-dimensional grid of electron densities suitable for ray tracing. Fourteen NIMS satellite passes were selected for which ionosonde measurements were available.

For each pass selected, OI ionograms were synthesized for the various paths by ray tracing through the five tomographic images created by methods A to E and three climatological models of electron density. The models used were the fully analytical ionospheric model (FAIM) [Anderson *et al.*, 1989], the parameterised ionospheric model (PIM) [Daniell *et al.*, 1995], and the international reference ionosphere model (IRI-95) [Bilitza *et al.*, 1993]. Each model was run to produce electron densities with grid intervals of 5 km in height, 0.25° in latitude, and 1° in longitude.

The synthetic ionograms created using the tomographic images and the ionospheric models were compared with the experimental IRIS oblique sounder ionograms on all six paths of the U.K. network. To quantify the level of agreement between the synthesized and measured traces, the six parameters identified in Figure 3 were scaled from each ionogram. These parameters were $f_{\min}(F)$, the minimum frequency of the F trace, $MUF(E)$ and $MUF(F_2)$, the maximum usable frequencies of the E and F_2 traces, respectively, and $m'd(E)$, $m'd(F_1)$, and $m'd(F_2)$, the minimum absolute time delay of

the E , F_1 , and F_2 traces, respectively. When no clear bifurcation of the F trace could be identified, the minimum delay was recorded as $m'd(F_1)$, and $m'd(F_2)$ was omitted.

4.1. MUF Comparisons

The results are presented from the ray tracing through each of the five tomographic specifications of the ionosphere and the three climatological models. The parameters determined from the resultant synthetic ionograms were differenced from the corresponding parameters obtained from the actual OI experimental observations. Average values and corresponding RMS errors were calculated for each of the OI parameter differences for all available paths and all of the 14 times of interest. The results are shown in the form of mean percentage overestimates of the parameter obtained using a tomographic or model specification of the ionosphere compared to that found experimentally. The mean percentage overestimates of the three frequency parameters scaled from the ionograms are shown in Figure 4, with the root-mean-square errors being plotted in Figure 5.

It can be seen that in every case the MUF of the E layer is underestimated, while that of the F region is overestimated. However, it can be noted that in tomographic reconstruction it would be expected that an underestimate of the E region peak density would be likely to result in a redistribution of plasma to

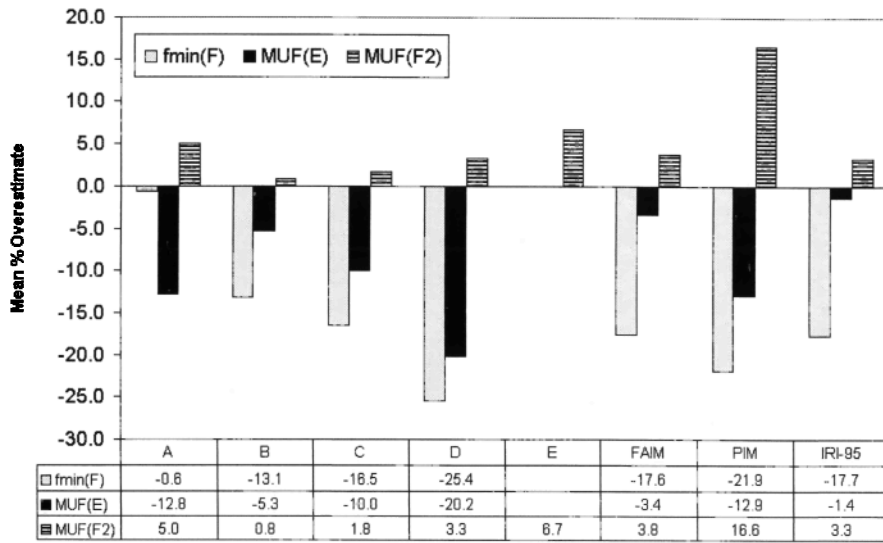


Figure 4. Mean percentage overestimates of $f_{\min}(F)$, $MUF(E)$, and $MUF(F_2)$ for tomographic imaging techniques A–E and ionospheric models FAIM, PIM, and IRI-95.

higher altitudes to yield the same TEC. Comparing the results from method A with those of method B, it is clear that the average difference between the estimated and the measured values of both $MUF(E)$ and $MUF(F_2)$ is smaller when the height interval of the tomographic grid is reduced from 15 km to 5 km. In addition, the $MUF(F_2)$ parameters for method B are in better agreement with those obtained experi-

mentally than the values predicted by use of the three climatological models, while the RMS errors are also significantly smaller. It can be seen that the inclusion of the data from the second ionosonde at Lerwick (method C) provided no improvement over method B, though the scatter of the differences as shown by the RMS errors was smallest in this case. When no vertical sounder information was used to constrain

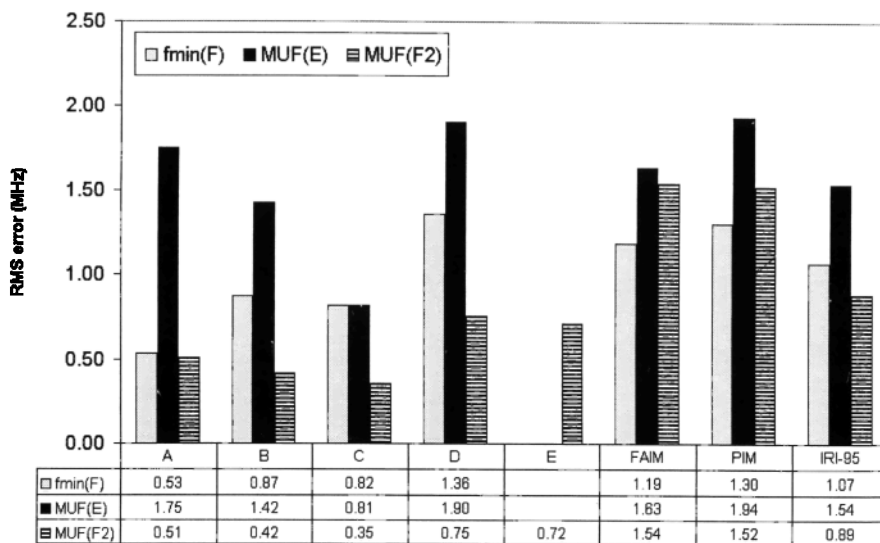


Figure 5. RMS errors in $f_{\min}(F)$, $MUF(E)$, and $MUF(F_2)$ for tomographic imaging methods A–E and ionospheric models FAIM, PIM, and IRI-95.

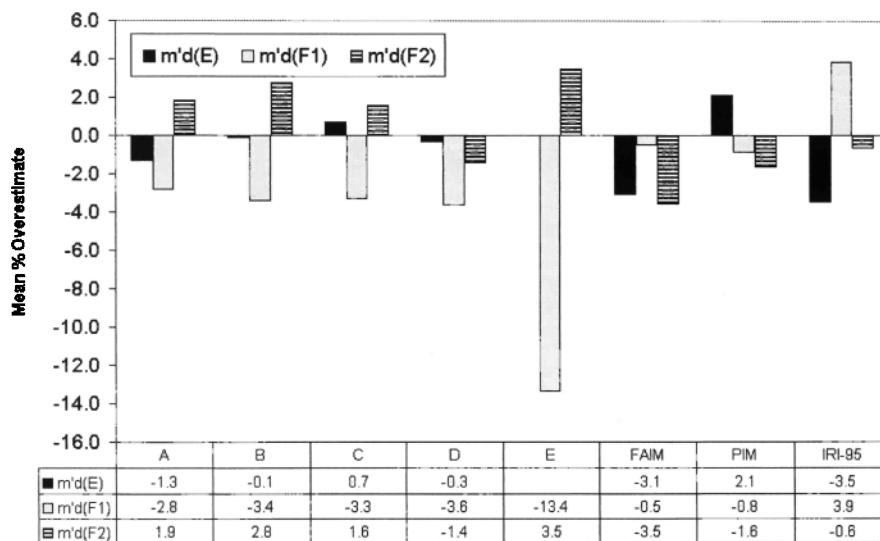


Figure 6. Mean percentage overestimates of $m'd(E)$, $m'd(F_1)$, and $m'd(F_2)$ for tomographic imaging techniques A–E and ionospheric models FAIM, PIM, and IRI-95.

the tomographic reconstruction (method D), it can be seen that there is a 20% underestimate of the E region MUF on average and large RMS errors in the frequency-scaled parameters.

For method E, in which only F region Chapman profiles were used in the reconstruction, the mean percentage overestimate of MUF(F_2) was significantly worse than that for method D. Thus it appears that even without VI ionosonde measurements, inclusion of some form of representation of the E region in the reconstruction process improves the usefulness of the tomographic image for HF applications.

It can be noticed from Figures 4 and 5 that the climatological FAIM and IRI-95 models both yield smaller average overestimates in MUF(E) than the best tomographic methods. Since the E region ionization at midlatitudes makes only a very small contribution to the overall TEC, the structure of this layer is inevitably poorly defined in any tomographic image. However, in HF oblique propagation, the path of the ray may be greatly affected by the E region, either acting as a reflector or defining the launch angle into the F region. The general behavior of the midlatitude E layer under solar control is well understood and modeled. Thus a possible practical approach to using tomographic imaging for ray tracing might be to employ a climatological model to specify the E region density while leaving the normal recon-

struction procedures to recreate the density structures of the F layer.

4.2. The $f_{\min}(F)$ Comparisons

The parameter $f_{\min}(F)$ is effectively a measure of the f_oE at the path midpoint and was only scaled when a clear frequency cutoff was observed (i.e., at the point of asymptotic group retardation). The $f_{\min}(F)$ was more difficult to scale on the longer paths. When using the tomographic images, the overestimates were found to be slightly reduced when ionosonde electron density profiles were included in the reconstruction (methods B and C) as compared with method D, though the improvement over the climatological models was still only marginal. The $f_{\min}(F)$ errors for tomographic method A were the lowest of all the ray tracing techniques.

4.3. Minimum Trace Delay Comparisons

Statistical comparisons of the minimum delay ($m'd$) of E , F_1 , and F_2 traces are presented in Figure 6 for the mean percentage overestimates and Figure 7 for the corresponding RMS errors. It can be seen that the mean percentage overestimates in $m'd(E)$ are smaller when a tomographic specification of the ionosphere was used than for the climatological models. The values of $m'd(F_1)$ were consistently underestimated by tomographic techniques, particularly for

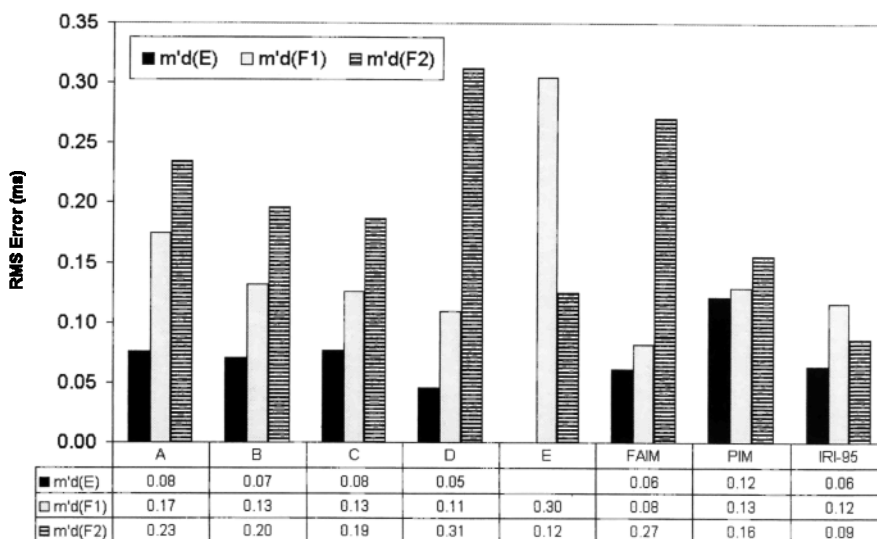


Figure 7. RMS errors in the minimum group delay of E , F_1 , and F_2 traces for tomographic imaging methods A–E and ionospheric models FAIM, PIM, and IRI-95.

method E, in which the reconstruction was based only on the F layer, whereas the underestimates obtained by use of the FAIM and PIM models were very small for this parameter. It thus seems likely that the tomographic reconstructions used here create images that are underdense in the E and/or E - F valley regions of the ionosphere, since higher densities would lead to greater group retardation. With regard to the $m'd(F_2)$ measurements there is an anticorrelation with errors in $m'd(F_1)$ in most of the tomographic methods.

5. Conclusions

The potential use of a number of radio tomographic reconstruction techniques to HF oblique propagation has been assessed by comparing synthesized oblique incidence ionograms with oblique ionograms recorded experimentally over six U.K. paths. Comparisons of ray-traced, synthetic oblique ionograms with real ionograms from the IRIS sounder network have shown the importance of using a fine height resolution and including electron density profiles deduced from vertical incidence ionosondes in the tomographic reconstruction process. While all of the reconstruction methods used here overestimated the F region MUFs, the tomographic techniques matched those recorded on the experimental OI ionograms much better than the MUFs based on models. However, the virtual height of the F region

tended to be underestimated when using the tomographic methods to specify the ionosphere, possibly as a consequence of the electron densities in the E and the E - F valley regions being consistently too low in the tomographic images.

It was found that the FAIM and IRI-95 models provided a better representation of the E region MUF than those estimated using the tomographic images. Thus it is suggested that in a practical application to an HF system a hybrid solution might be found, whereby a climatological model might be used to represent the E region as an input to the reconstruction process with the tomographic techniques being used to provide a reliable description of the latitudinal structure of the F region.

Acknowledgments. This research is supported by the Corporate Research Programme of the U.K. Ministry of Defence. The ionospheric models FAIM and PIM were provided by Computational Physics, Norwood, Massachusetts, and the U.S. Air Force Research Laboratory, Hanscom Air Force Base, Massachusetts. The IRI-95 model was provided by the U.S. National Space Science Data Center (NSSDC). We are grateful to the World Data Centre at the Rutherford Appleton Laboratory, England, United Kingdom, for supplying vertical incidence ionosonde data. The contributions to this project by other members of the Radio and Space Physics Group at Aberystwyth, and in particular the technical assistance of Clive Willson, are acknowledged with thanks.

References

- Anderson, D. N., J. M. Forbes, and M. Codrescu, A fully analytic, low and middle latitude ionospheric model, *J. Geophys. Res.*, *94*, 1520–1524, 1989.
- Arthur, P. C., M. Lissimore, P. S. Cannon, and N. C. Davies, Application of a high quality ionosonde to ionospheric research, in *IEE 7th International Conference on HF Radio Systems and Techniques*, *IEE Conf. Publ.*, *441*, 135, 1997.
- Bilitza, D., K. Rawer, L. Bosny, and T. Gulyaeva, International reference ionosphere: Past, present and future, 1, Electron density, *Adv. Space Res.*, *13*(3), 3–13, 1993.
- Daniell, R. E., Jr., L. D. Brown, D. N. Anderson, M. W. Fox, P. H. Doherty, D. T. Decker, J. J. Sojka, and R. W. Schunk, PIM: A global ionospheric parameterization based on first principles models, *Radio Sci.*, *30*, 1499–1510, 1995.
- Dyson, P. L., and J. A. Bennett, A model of the electron concentration with height in the ionosphere and its application to oblique propagation studies, *J. Atmos. Terr. Phys.*, *50*(3), 251–262, 1988.
- Fremouw, E. J., J. A. Secan, and B. M. Howe, Application of stochastic inverse theory to ionospheric tomography, *Radio Sci.*, *27*, 721–732, 1992.
- Kersley, L., S. E. Pryse, I. K. Walker, J. A. T. Heaton, C. N. Mitchell, M. J. Williams, and C. A. Willson, Imaging of electron density troughs by tomographic techniques, *Radio Sci.*, *32*, 1607–1621, 1997.
- Leitinger, R., Ionospheric tomography, in *Review of Radio Science, 1996–1999*, edited by W. R. Stone, chap. 24, pp. 581–623, Oxford Univ. Press, New York, 1999.
- Leitinger, R., G. Schmidt, and A. Tauriainen, An evaluation method combining the differential Doppler measurements from two stations that enables the calculation of the electron content of the ionosphere, *J. Geophys.*, *41*, 201–213, 1975.
- Norman, R. J., and P. S. Cannon, A two-dimensional analytical ray tracing technique accommodating horizontal gradients, *Radio Sci.*, *32*, 387–396, 1997.
- Norman, R. J., and P. S. Cannon, An evaluation of a new two-dimensional analytic ionospheric ray-tracing technique (SMART), *Radio Sci.*, *34*, 489–499, 1999.
- Pryse, S. E., L. Kersley, C. N. Mitchell, P. S. J. Spencer, and M. J. Williams, A comparison of reconstruction techniques used in ionospheric tomography, *Radio Sci.*, *33*, 1767–1779, 1998.
- Rogers, N. C., P. S. Cannon, J. A. T. Heaton, C. N. Mitchell, and L. Kersley, Ray tracing through tomographic images of the ionosphere, in *IEE National Conference on Antennas and Propagation*, *IEE Conf. Publ.*, *461*, 345–348, 1999.
- Titheridge, J. E., Increased accuracy with simple methods of ionogram analysis, *J. Atmos. Terr. Phys.*, *41*, 243–350, 1979.
- Titheridge, J. E., Ionogram analysis with the generalised program POLAN, *Rep. UAG-93*, Univ. of Auckland, Auckland, N. Z., 1985.
- P. S. Cannon, J. A. T. Heaton, and N. C. Rogers, Radio Science and Propagation Group, QinetiQ, Malvern, Worcestershire WR14 3PS, England, U.K. (pcannon@qinetiq.com; jheaton@qinetiq.com; nrogers@qinetiq.com)
- L. Kersley, Department of Physics, University of Wales, Aberystwyth, Ceredigion SY23 3BZ, Wales, U.K. (lek@aber.ac.uk)
- C. N. Mitchell, Department of Electronic and Electrical Engineering, University of Bath, Bath BA2 7AY, England, U.K. (eescnm@bath.ac.uk)

(Received June 1, 2000; revised May 23, 2001; accepted May 29, 2001.)